A Facile Route to Targeted, Biodegradable Polymeric Prodrugs for the Delivery of Combination Therapy for Malaria

Lisa Fortuin[†], Meta Leshabane[§], Rueben Pfukwa[†], Dina Coertzen[§], Lyn-Marie Birkholtz[§], Bert Klumperman[†]**

[†]Department of Chemistry and Polymer Science, Stellenbosch University, Private Bag X1, Matieland 7602, South Africa

[§] Department of Biochemistry, Genetics and Microbiology, Institute for Sustainable Malaria Control, University of Pretoria, Private Bag X20, Hatfield 0028, South Africa.

ABSTRACT: A facile synthetic methodology has been developed to prepare multi-faceted polymeric prodrugs that are targeted, biodegradable and non-toxic, used for the delivery of a combination therapy. This is the first instance of the delivery of the WHO recommended antimalarial combination of lumefantrine (LUM, drug 1) and artemether (AM, drug 2) via a polymeric prodrug. To achieve this, RAFT-mediated polymerization of *N*-vinylpyrrolidone (NVP) was conducted using a hydroxy-functional RAFT agent, and the resulting polymer used as the macroinitiator in the ring-opening polymerization (ROP) of α-allylvalerolactone (AVL) to synthesize the biodegradable block copolymer of poly(*N*-vinylpyrrolidone) and poly(α-allylvalerolactone) (PVP-*b*-PAVL). The ω-end thiol group of PVP was protected using 2,2'-pyridyldisulfide prior to the ROP, which was conveniently used to bioconjugate a peptidic targeting ligand. To attach LUM, the allyl groups of PVP-*b*-PAVL underwent oxidation to introduce carboxylic acid groups, which were then esterified with ethylene glycol vinyl ether. LUM was lastly conjugated to the block copolymer via an acid-labile acetal linkage in a 'click'-type reaction and AM was entrapped within the hydrophobic core of the self-assembled aggregates to render the biodegradable multi-drug loaded micelles for combination therapy with targeting ability.

Drug delivery; polymeric prodrug; nanomedicine; combination therapy; malaria

INTRODUCTION

Polymeric prodrugs, i.e. covalently linked polymer-drug conjugates, are a key element in the very important field of polymer therapeutics.[1, 2] They have progressed significantly from the original polymeric prodrug introduced by Ringsdorf,[3] to modern systems based on amphiphilic block copolymer (BCP) micelles, which can also be classified as polymeric prodrugs if the drugs are covalently bound to the BCP polymeric carrier.[4-6] As with small molecule surfactants, amphiphilic BCPs also self-assemble into nanosized core-shell micelles, with a hydrophobic core surrounded by a hydrophilic shell. Polymer based micelles, however, are more stable.[7-9] The BCPs are usually composed of hydrophilic and hydrophobic block segments, the characteristic lengths of which determine the micelles' physiochemical properties. Ideal micellar carriers should demonstrate biocompatibility, a high drug loading capacity, stability and controlled drug release.[6, 8] The hydrophobic drugs are conjugated to the hydrophobic segment, and upon self-assembly into micelles, the drugs are located in the micelle core. Use of micellar polymeric prodrugs increases the aqueous solubility and stability of hydrophobic drugs, prolonging blood circulation[10] and improving biodistribution.[8] Also, nanosized micellar polymeric prodrugs have the ability to specifically target tissues or cells via active or passive mechanisms, resulting in lower off-target toxicities and improved therapeutics.[8, 11] At the site of action, specific events are initiated which ultimately lead to the activation of the therapeutic agent at the targeted site.[1, 2, 6]

Modern polymer synthesis techniques such as reversible addition-fragmentation chain transfer (RAFT)-mediated polymerization and ring-opening polymerization (ROP) have been instrumental in the development of well-defined polymers with predictable molecular weights, low molar mass dispersity ($Đ$) and tailored functionalities in pendant or terminal positions.[12, 13] This has enabled access to a wide range of functional amphiphilic BCPs for use in nanomedicine. Several polymers have been used as hydrophilic block segments, including polyethylene glycol (PEG), poly(vinyl alcohol) (PVA) and poly(*N*-vinylpyrrolidone) (PVP).[6, 8] We are particularly interested in PVP

based BCPs due to PVP's excellent water solubility, biocompatibility, chemical stability and facile polymerizability into well defined, end-functional polymers via the RAFT process.[14-20] Hydroxy-functional RAFT agents give rise to telechelic PVP-OHs with readily accessible thiols and -OH functionalities that can initiate ROPs with core forming blocks. Functional hydrophobic core forming blocks have been prepared from polypeptides,[21, 22] polyesters[23, 24] and vinyl polymers.[6, 8] Polypeptide and polyester based systems have the additional benefit of being degradable through hydrolysis into benign, excretable small molecules.[25, 26] Polyesters display an enhanced encapsulation of hydrophobic drugs, and form thermodynamically and kinetically stable micelles. Poly(δ-valerolactone) (PVL), a biodegradable, biocompatible aliphatic polyester, is relatively unexplored compared to poly(ϵ-caprolactone) (PCL), despite having similar physicochemical properties and shorter degradation times than the more commonly used PCL. In fact, PVL is comparable and exceeds PCL in certain aspects as a component of polymeric drug delivery devices.[27-29] The lactone monomers for PVL and PCL are also functionalizable, enabling the synthesis of polyesters with pendant reactive handles applicable in biomedicine.[30-33] In light of this, amphiphilic BCPs composed of PVP and PVL derivatives are potentially appealing for preparing polymer-drug conjugates, in particular for complex systems such as combination therapy.

Combination therapy, which is the simultaneous administration of two or more drugs, can bring about synergistic effects and help to limit the occurrence of drug resistance, by using drugs with complementary mechanisms of action which control different signaling pathways, minimizing adverse effects and leading to better long-term prognosis.[25, 34, 35] Combination therapy is being used to combat malaria in order to prevent the emergence of resistant organisms.[36] Malaria, the world's most prevalent parasitic disease, is caused by species of *Plasmodium, with P. falciparum* the most lethal species associated with mortality in Africa.[37] There is continued need for new malaria treatments due to *Plasmodium*'s alarming gain in resistance to antimalarials. Some therapeutics are associated with poor intrinsic characteristics (low water solubility and low stability) and may

require complex administration routes.[37-39] There are increasing efforts to treat malaria using nanosized assemblies of polymeric prodrugs to capitalize on the benefits of nanomedicines, which include improvements in the stability and water solubility of hydrophobic drugs. Target-specific delivery may allow for the use of potentially toxic antimalarials, and help to rejuvenate old drugs.[40, 41] The combination of artemether (AM) and lumefantrine (LUM), known as AL (CoArtem™), is currently recommended by the World Health Organization for the treatment of uncomplicated malaria due to the different yet synergistic modes of action which eradicate parasitemia and impede drug resistance.[36, 42] AM, with its short plasma half-life, rapidly eliminates parasitemia with LUM eliminating any residual parasitemia over longer times. The combined treatment, however, is complex, requiring 2 doses per day along with fat-coadministration to improve the absorption of the lipophilic LUM.[43] To the best of our knowledge, this drug combination has never been delivered using nanocarriers. This may help to solve issues around LUM's poor uptake as well as AM's short plasma half-life and low stability.

Herein, simple methods were used to develop a biodegradable, targeted, non-toxic polymeric prodrug based on PVP and a derivative of poly(δ-valerolactone) (PVL) functionalized with ethylene glycol vinyl ether (VE), i.e. PVP–PVL/VE BCPs, for the delivery of the AM and LUM antimalarial drug combination. The BCP was prepared by first synthesizing α-hydroxy end-functional PVP via RAFT-mediated polymerization, before using this as a macroinitiator in the ROP of α-allylvalerolactone (AVL). The allyl groups were then converted to carboxylic acid groups, before esterification with ethylene glycol vinyl ether (EGVE) to yield a reactive BCP scaffold bearing vinyl ether pendant groups. LUM was easily attached by acetalization, forming the polymer drug conjugate with acid-labile acetal polymer-drug linkers. Subsequent aqueous self-assembly, with core-entrapment of AM, then resulted in the formation of a nanocarrier for AM and LUM, and subsequent focus was placed on drug release and *in vitro* studies.

RESULTS AND DISCUSSION

Synthesis of the biodegradable block copolymer. α-Hydroxy end-functional PVP (PVP-OH) was synthesized via the redox-initiated aqueous RAFT polymerization of NVP using the xanthate chain transfer agent (CTA), 2-hydroxyethyl 2-(ethoxycarbonothioylthio)propanoate, bearing a hydroxy-functional R-group (Scheme 1). Although RAFT-mediated polymerization controls a wide monomer range, it is important to choose an appropriate CTA by careful selection of the Z- and R-group of the CTA in order to achieve successful control over the polymerization. Xanthates are generally well-suited for the less-activated monomers such as NVP.[44, 45] The synthesis of well-defined polymers with low *Đ* values in the range of 1.1 and good RAFT end group fidelities (>95%) was achieved, as confirmed via ^{1}H NMR spectroscopy (Figure S1, Table 1). Conversions were very high – to near quantitative (> 90%, Table 1). Polymer kinetics are shown in Figure S2 in the SI. The ω-xanthate end group of the PVP-OH was converted to a pyridyl disulfide (PDS)-protected thiol to limit side-reactions which could occur during the subsequent ROP and post-polymerization reactions. For example, xanthate Z-groups can be aminolyzed by the base catalysts used for ROP.[46] Such aminolysis reactions can produce free thiols which can also initiate ROP,[47] and would likely react with the allyl-functional valerolactone via thiol-ene coupling. Moreover, the PDS group provides an efficient functional handle onto which a thiol-bearing targeting ligand can be attached once the polymeric prodrug is assembled. This was accomplished by aminolyzing the ω-xanthate end group using ethanolamine in the presence of excess 2,2'-pyridyldisulfide,[48] to effect the ω-end group modification in one pot, accessing PDS-terminated PVP-OH (PDS-PVP-OH) in near-quantitative conversions (Scheme S4). The successful synthesis of PDS-PVP-OH was confirmed by the appearance of the characteristic signals of the pyridyl ring at δ 8.4, 8 – 7.6 and 7.3 ppm in the ^{1}H NMR spectrum (Figure 1a). PDS is insoluble in water so the appearance of its characteristic aromatic signals signifies that it was solubilized by attachment to the polymer's chain end. SEC analysis before and after end group modification showed that the polymers had similar molar

masses and monomodal distributions indicating that there was no disulfide coupling between polymer chains (Figure 1b).

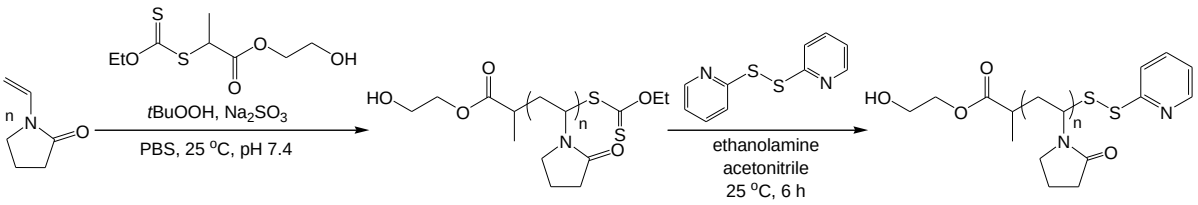

Scheme 1. Synthesis route to PVP-OH and subsequent thiol-protected PDS-PVP-OH.

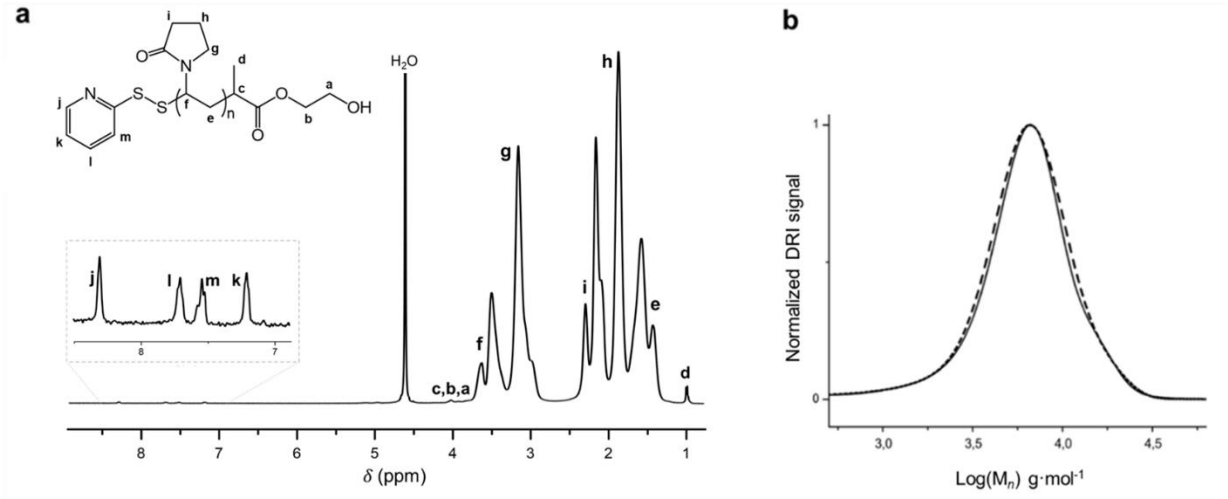

Figure 1. a) ^{1}H NMR spectrum of PDS-PVP-OH (D_2O, 400 MHz) and b) overlaid molar mass distribution curves of PVP-OH (solid line) and PDS-PVP-OH (dashed line) (run 1 and 2, Table 1).

Table 1. Synthesis and analytical details of PVP-OH and PDS-PVP-OH

Polymer	∝ / yield [a]	Time	Temperature	$M_{n,target}$ [b]	$M_{n,SEC}$ [c]	$M_{n,NMR}$ [d]	f_{RAFT} [e]	$Đ$
	%	h	°C	g·mol^{-1}	g·mol^{-1}	g·mol^{-1}	%	
PVP-OH	90[#]	6	25	4000	4000	3900	98	1.1
PDS-PVP-OH*	99	24	25	-	4000	3900	-	1.1
PVP-OH	91[#]	6	25	12 000	11 800	11 200	96	1.1
PDS-PVP-OH*	96	24	25	-	11 800	11 100	-	1.1

[a] Gravimetric yield, which also reflects gravimetric conversion of NVP to PVP-OH[#], [b] $M_{n,target}$ is the targeted molar mass (Equation S1), [c] $M_{n,SEC}$ is based on PMMA standards, eluent DMF, [d] $M_{n,NMR}$ is determined by the ratio of integral signals of the xanthate end group to polymer backbone (Equation S2), [e] f_{RAFT} is the RAFT end group fidelity (Equation S3), *PDS-PVP-OH prepared from immediately preceding PVP-OH.

The homo- and copolymerization of AVL with ε–caprolactone via stannous octanoate catalyzed ROP, has been reported.[33] The allyl functionalities provide unique opportunities for further modification of AVL-based copolymers. Herein, AVL was synthesized according to the procedure by Molander and Harris, by treating δ–valerolactone (VL) with lithium *N,N*-diisopropylamide followed by allylbromide.[49] The structure was confirmed by NMR and mass spectrometry (see SI).

The organocatalytic anionic ROP of lactones is typically conducted with the guanidine organocatalyst 1,5,7-triazabicyclodecene (TBD) or the amidine organocatalyst 1,8-diazabicycloundec-7-ene (DBU).[50] Towards preparing well-defined PVP-PAVL BCPs, we investigated optimum conditions for the organocatalytic ROP (OCROP) of AVL with TBD and DBU, and compared this to the known OCROP of VL.[51] The polymerization conditions of VL using 1-pyrenemethanol (1-PM) as the initiator with the organocatalysts TBD (run 1), DBU + TU (run 2) and DBU (run 3) are shown in Table 2. Lohmeijer et al. showed that TBD has a unique ability to simultaneously activate both the alcohol and the monomer, whereas DBU can only activate the alcohol, and required a cocatalyst for the ROP of VL.[51]

Table 2. Polymerization and analytical details of PVLs, PVP-*b*-PVLs and PVP-*b*-PAVLs

Polymer	Cat. [a]	Cat. loading	Time h	End group retention	$\propto$ [b] %	$M_{n,target}$ [c] g·mol^{-1}	$M_{n,SEC}$ [d] g·mol^{-1}	$M_{n,NMR}$ [e] g·mol^{-1}	$Đ$ [f]
PVL	TBD	2 mol%	0.1	~1	95	5200	4900	5300	1.1
PVL	DBU + TU	5 mol%	3	~0.5	82	5200	4100	4100	1.2
PVL	DBU	5 mol%	24	n.d [f]	22	5200	2300	n.d [f]	1.2
PAVL	TBD	2 mol%	0.1	~1	89	5200	4500	4300	1.1

Label [g]	Copolymer composition [h]	$M_{n,theoretical}$ [i] g·mol^{-1}	$M_{n,SEC}$ [j] g·mol^{-1}	f_{phil} [k]	$Đ$ [f]
BCP1	PVP_{27}-*b*-PVL_{53}	5880	8300	0.3	1.1
BCP2	PVP_{138}-*b*-PVL_{100}	22 5040	25 400	0.6	1.2
BCP3	PVP_{138}-*b*-PVL_{346}	35 000	41 400	0.4	1.2

BCP4	PVP_{36}-*b*-$PAVL_{35}$	7800	9300	0.5	1.2
BCP5	PVP_{138}-*b*-$PAVL_{63}$	18 800	24 100	0.7	1.2

[a] 'Cat.' is 'organocatalyst' and DBU:TU is 1:1. [b] conversion of VL or AVL to PVL or PAVL, respectively, determined gravimetrically, [c] $M_{n,target} = \left(\frac{[monomer]}{[initiator]}\right) \cdot \propto \cdot M_{r,monomer} + M_{r,initiator}$ where $\propto = 1$ for 100% conversion, [d] $M_{n,SEC}$ is determined by SEC based on polystyrene standards, eluent THF, [e] $M_{n,NMR}$ is determined by ^{1}H NMR in $CDCl_3$ as the ratio of the signals *a* of pyrene to *e* of the polymer backbone (Figure 3) [f] $Đ$ represents the dispersity from SEC (M_w / M_n), [f] n.d is not determined. [g] The organocatalyst is TBD (2 mol%) and proceeded to completion within 0.2 h, [h] estimated from SEC, [i] $M_{n,theoretical} = \left(\frac{[monomer]}{[macroinitiator]}\right) \cdot \propto \cdot M_{r,monomer} + M_{r,macroinitiator}$ where $\propto$ is the gravimetric conversion, [j] $M_{n,SEC}$ is determined by SEC based on PMMA standards, eluent DMF, [k] f_{phil} is the hydrophilic fraction estimated from the copolymer composition. All polymerizations and were conducted at 25 ºC.

The homopolymers were analyzed by ^{1}H NMR spectroscopy (Figure 2). Characteristic signals for the α- chain end (methylene protons **f** at 5.8 ppm) and for the ω-chain end (methylene protons **b** at 3.6 ppm) were used to calculate the end group retention values in Table 2. With TBD catalysis (Figure 2a), the ideal integral ratio of α:ω end groups of ~1 was obtained, however, with DBU+TU (Figure 2b) a ratio of ~0.5 was obtained. DBU is a competent nucleophile, and has been shown to initiate the ROP of lactides and cyclic anhydrides in the absence of alcohol initiators,[52-55] by nucleophilically attacking the cyclic monomers' carbonyl carbon, generating a zwitterionic propagating species.[56, 57] It is likely that DBU also initiates the ROP of VL since signals assignable to DBU are observed in the spectra of PVL as seen in Figure 2b. This would account for the discrepancy in the retention of the desired α:ω end groups observed via ^{1}H NMR spectroscopy, with a fraction of the chains being initiated by 1-PM, and another by DBU, and also the slight increase in $Đ$. DBU based ROPs also proceeded to lower conversions in much longer reaction times, indicating more sluggish kinetics than in the case of TBD catalysis. Based on this, to avoid the DBU complications, TBD was used to promote the ROPs of VL and AVL in the block copolymer synthesis. Polymerizations of the block copolymers (BCPs, Table 2) proceeded to reasonably high conversions in short reaction times. Figures 3b and S4 show the molar mass distribution curves and ^{1}H NMR spectrum of PVP-*b*-PAVL, respectively. PVP-OH was successfully chain extended with VL (Figure 3) and AVL, confirming the versatility of this system.

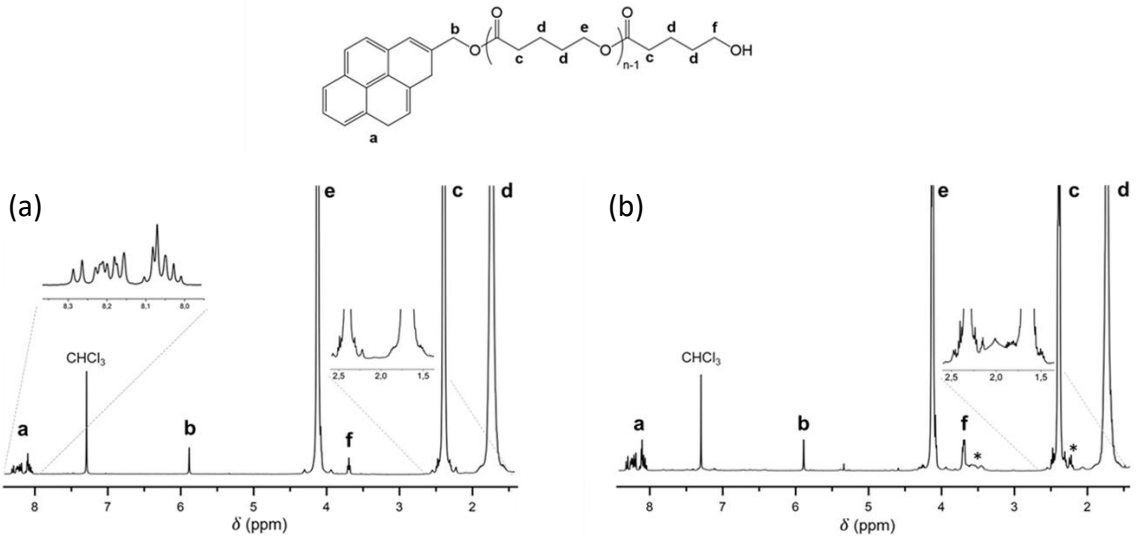

Figure 2. ^{1}H NMR spectra of PVLs synthesized with a) TBD and b) DBU + thiourea catalysis ($CDCl_3$, 400 MHz).

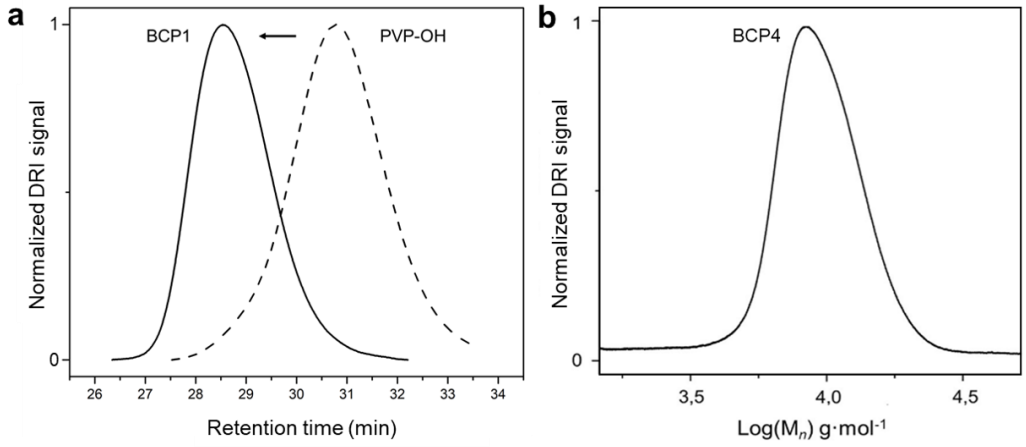

Figure 3. a) Representative SEC chromatograms of PVP-OH and BCP1 and b) the molar mass distribution curve of BCP4.

Modification and drug conjugation. The polymer-drug conjugate was prepared in three steps (Scheme 2) using PVP-*b*-PAVL (BCP4, Table 2). In the first step, the pendant allyl groups were quantitatively oxidized to carboxylic acid groups in a biphasic medium composed of DCM and acetic acid with $KMnO_4$ in the presence of 18-crown-6.[58] The successful reaction was confirmed by ^{1}H NMR spectroscopy which showed the complete removal of PVP-*b*-PAVL's vinyl signals 5.7 ppm (=CH−) and at 5.0 ppm (=CH_2) (Figure 4a and 4b) and ^{13}C NMR spectroscopy (Figure S5),

which showed the appearance of −COOH carbon. Subsequently, EGVE moieties were attached to the polyester block via the Steglich esterification with the pendant COOH functionalities to access the vinyl ether functionalized BCP. EGVE functionalization was confirmed using ^{1}H NMR spectroscopy (~70 mol%), with the signals attributed to EGVE's vinyl and methylene protons appearing between 6.5 – 3.5 ppm (Figure 4c). In the last step, LUM was conjugated to EGVE-functionalized PVP-*b*-PAVL via acid-labile acetal linkages through a 'click'-type reaction between the hydroxy group of LUM and the pendant vinyl ether groups.[59] Figure 4d shows the ^{1}H NMR spectrum of the LUM-functionalized block copolymer (22 mol%).

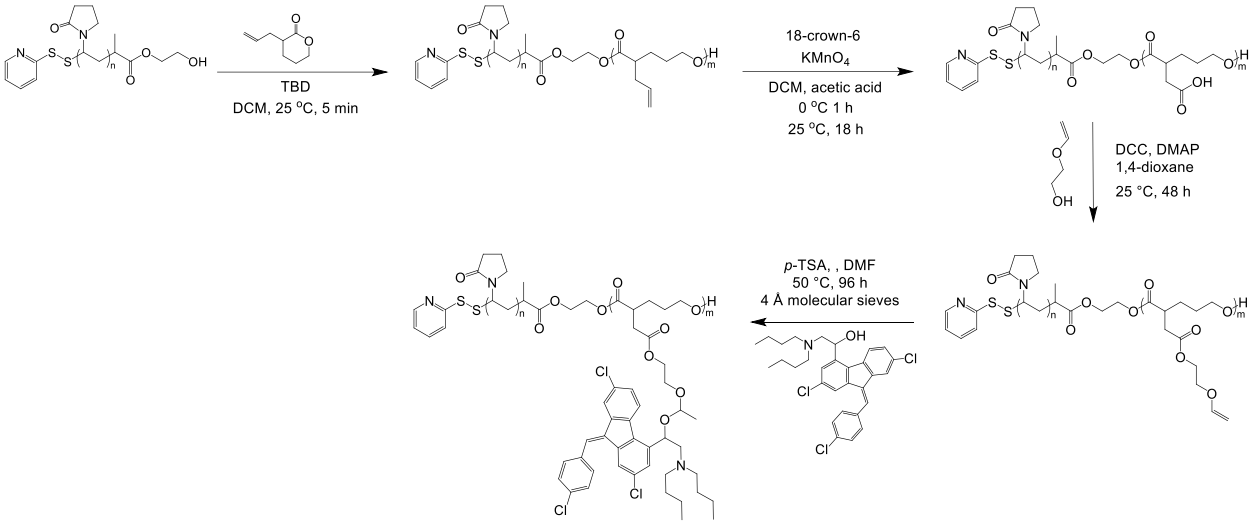

Scheme 2. Synthesis route to the LUM prodrug.

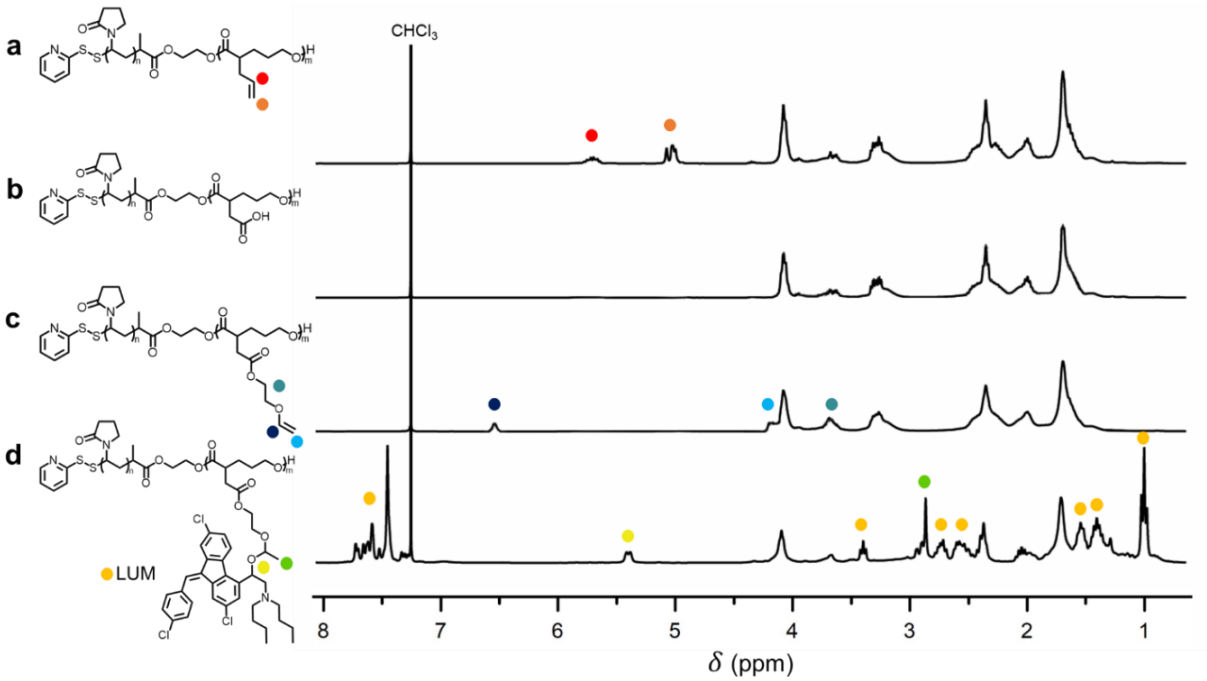

Figure 4. ^{1}H NMR spectra and chemical structures of a) PVP-*b*-PAVL, b) carboxylated PVP-*b*-PVL, c) EGVE-functionalized PVP-*b*-PVL and d) LUM prodrug ($CDCl_3$, 400 MHz).

The SEC curve of the LUM prodrug was monomodal and symmetrical (Figure 5a, $Đ$ = 1.4), indicative of one molar mass distribution. Diffusion-ordered NMR spectroscopy (DOSY) was used to provide further evidence of successful LUM conjugation to the BCP. DOSY analysis produces two-dimensional correlation maps with chemical shifts on the horizontal axis and diffusion coefficients on the vertical axis. NMR signals of nuclei on the same molecule are correlated with the same diffusion coefficient, in the absence of intermolecular interactions or chemical exchange, allowing for the differentiation of NMR signals produced by molecules with different sizes.[60, 61] Figure 5b shows the DOSY map of the polymer-drug conjugate; the resonances of the BCP backbone and the LUM drug have the same translational mobility, indicating that they are linked together and that drug conjugate formation was successful.

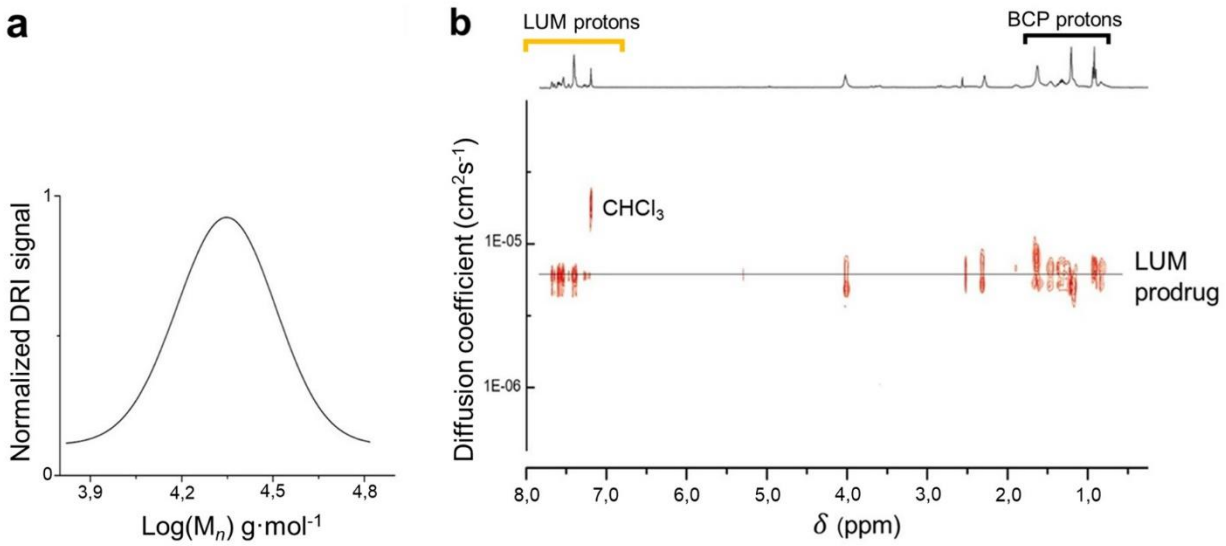

Figure 5. a) Molar mass distribution from SEC and b) DOSY spectrum of the LUM prodrug.

Preparation and characterization of AM loaded polymer-prodrug micelles. AM, drug 2, is a poorly water soluble drug with a solubility of 114 mg·L^{-1} at pH 7.0. Poor water solubility of drugs is one of the most critical problems in drug development, as water solubility influences drug pharmacokinetics and pharmacodynamics.[62] This limitation can be overcome by encapsulating drugs inside BCP micelles,[6, 8] and this approach was used herein to entrap AM within the hydrophobic core of LUM prodrug micelles. The drug loaded micelles (DLMs) were prepared by dissolving the BCP-LUM conjugates and AM in THF, followed by the slow addition of water, a non-solvent for both the hydrophobic LUM functionalized polyester block and AM, to drive micelle formation by self-assembly. TEM analysis of DLMs (Figure 6a) revealed the formation of uniform spherical aggregates with diameters of ~25 nm. Analysis by dynamic light scattering (DLS) corroborated the presence of assemblies (Figure 6b), however, with a diameter of ~114 nm, much larger than deduced from TEM. This discrepancy is largely as a result of drying effects encountered with TEM, as the aggregates are dried under vacuum and are measured in the dry state, compared to the solvent-swollen aggregates measured using DLS. The size of the DLMs is above the upper limit (70 nm) described for passive targeting of *Plasmodium* infected red blood cells,[63]

via the so-called new permeation pathways (NPPs), which impart an enhanced permeability to infected red blood cells (iRBCs) post invasion. It has been established that macromolecules and nanoparticles can gain access to the intracellular parasite, without going through the host cytosol through various types of NPPs.[64, 65] It is not clear, however, which mechanism (or combination of mechanisms) enables the delivery of antimalarials into infected red blood cells.[66] Nonetheless, there is an increasing number of reports seeking to capitalize on this iRBC 'leakiness' to enable the uptake of polymer prodrugs and drug loaded nanoparticles into iRBCs for antimalarial chemotherapy.[67]

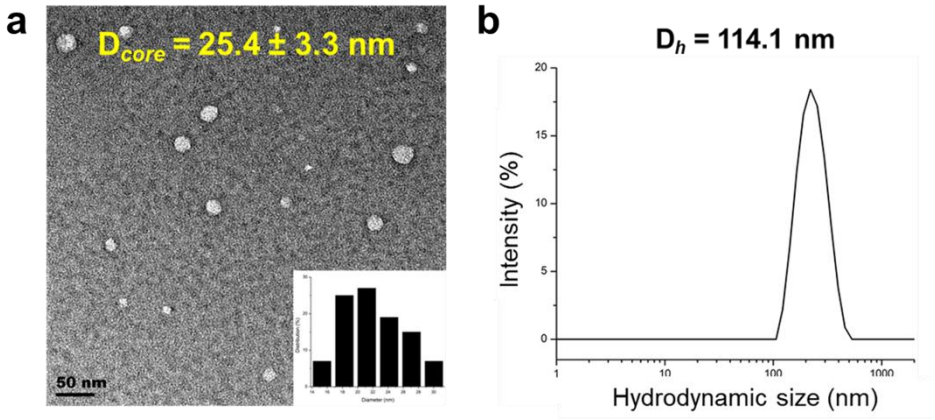

Figure 6. a) TEM image with the average size (D_{core}) and size distribution, and b) DLS curve with the average hydrodynamic size (D_h) of DLMs.

Figure 7 shows the DSC endotherms of AM and the DLM. Pristine AM exhibits a melting endotherm at 88.1 °C, ΔH: 61.2 $J \cdot g^{-1}$, consistent with literature values between 86 – 90 °C.[68] The DLM, however, does not exhibit this melting endotherm, suggesting that the entrapped AM is in a dispersed state in the DLM core. Crystalline drugs dissolve and diffuse slowly into the outer aqueous environment, influencing drug release kinetics.[69] LC-MS analysis showed that the drug loading content (DLC) and entrapment efficiency (EE) of AM in the DLM was 14 wt.% and 60%, respectively, and the DLC of LUM in the DLM was 27 wt.%. The DLCs obtained here compare favorably against known values of hydrophobic drugs which are often between 5 - 25 wt.%.[9, 30] In

fact, lower DLCs (<10 wt.%) have been reported for BCP drug delivery systems with semicrystalline core forming blocks, where the crystallinity limited the solubility of the hydrophobic drugs within the micelle cores.[70, 71]

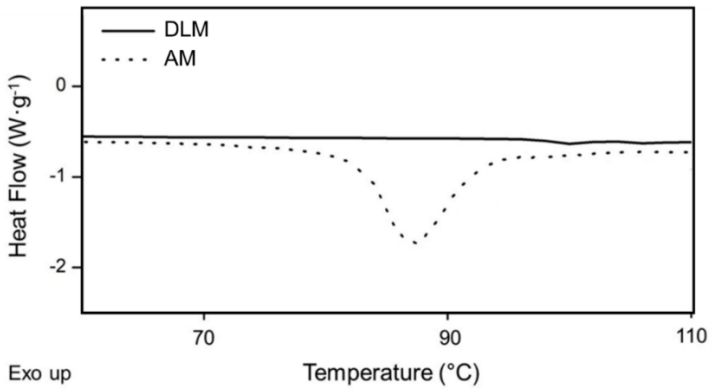

Figure 7. DSC thermograms of AM (dotted curve) and DLM (line curve) over the characteristic melting endotherm area of crystalline AM. Second heating cycle shown.

The critical micelle concentration (CMC) is the threshold at which unimers assemble into micelles, therefore, the lower the CMC value, the more thermodynamically stable the micelles. The CMC of the DLMs was measured by fluorimetry using pyrene as a probe,[72] (Figure 8a) and was found to be 2.0×10^{-3} mg·mL^{-1}. For a comparison, the CMC of empty micelles (EM) assembled from PVP-*b*-PAVL of the same composition, was found to be 5.2×10^{-3} mg·mL^{-1}, indicating greater thermodynamic stability for the DLMs. Drug-core interactions are known to enhance the thermodynamic stability of block copolymer nanostructures.[73]

The kinetic stability of the DLMs was investigated by measuring the average hydrodynamic diameter of the aggregates as a function of time, in phosphate buffered saline (PBS) and in PBS/fetal bovine serum (to mimic physiological conditions), at 37 °C (Figure 8b). The stability of polymer prodrug micelles in the physiological environment is a major concern, as destabilization by opsonin proteins in blood plasma is known to occur *in vivo*.[74] The DLMs were found to be stable for five days in PBS and four days in PBS/FBS as after this time, dissociation into unimers likely

occurred. Another indication of micelle instability is the formation of multi-modal aggregates with larger hydrodynamic volumes, more commonly observed for DLMs in PBS (2100 nm after 14 days, data not shown). PVP hydrophilic chains presumably 'shielded' the hydrophobic core (composition 1:1 wt. fraction) allowing for prolonged micelle stability in aqueous media. Micelles were likely destabilized more quickly in PBS/FBS due the aforementioned serum proteins, able to adsorb on the DLMs to accelerate the destabilization process after a critical point.[72]

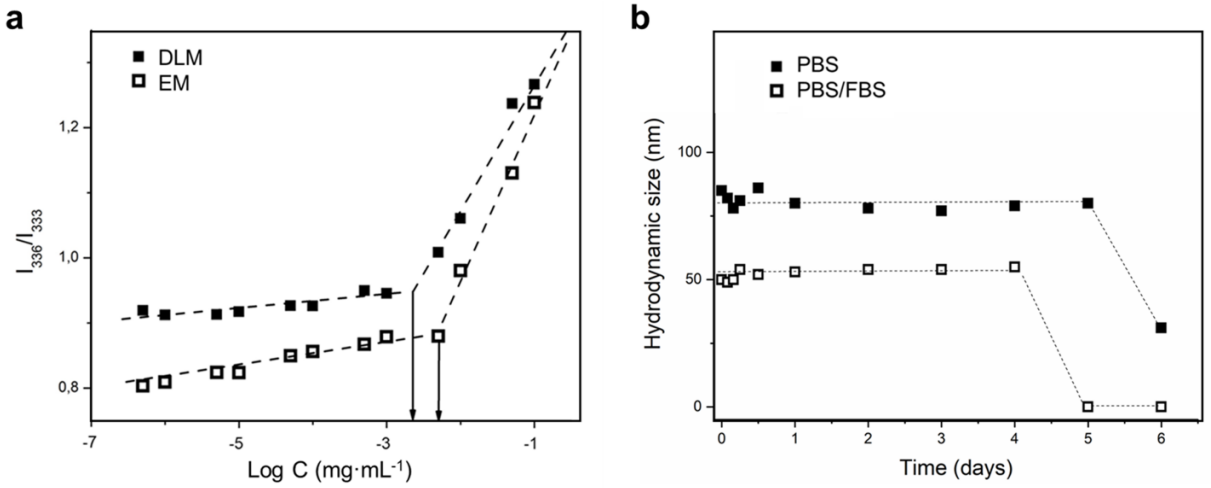

Figure 8. a) Fluorescence intensity of $I_{337\ nm}/I_{333\ nm}$ for pyrene as a function of the logarithm of concentration of micelles self-assembled from EMs and DLMs, and b) the kinetic stability of DLMs at 37 °C in PBS (pH 7.4) and PBS/FBS over several days.

After the invasion of an RBC by the *Plasmodium* parasite, it endocytoses and digests two-thirds of the host cell's contents within its acidic food vacuole, which appears to be a non-discriminative process without the need for receptors to bind particular substrates.[75] The ability of the drug delivery system to remain stable in neutral media and degrade in acidic media is important because the system is designed to degrade and release the drugs in low pH environments similar to the ones present in the parasite's food vacuole,[76] upon uptake. The drug release from the DLM was studied in a PBS buffer (pH 7.4) and in an acetate buffer (pH 5) at 37 °C using the dialysis technique. The cumulative% drug release curves of LUM and AM are shown in Figure 9a and b, respectively.

After three days, approximately 70±5% of LUM and AM had been released at pH 5.0 compared to ~20% at pH 7.4. Importantly, the drug release was enhanced under acidic conditions and no burst release had occurred. Burst release is a phenomenon whereby an initial, large bolus of drug is released before the release rate can become stable. It could be harmful to the patient due to the toxicity of the drug(s) exposed to healthy organs and tissues, and could also lead to a reduction in the system's lifetime, reducing its economic viability.

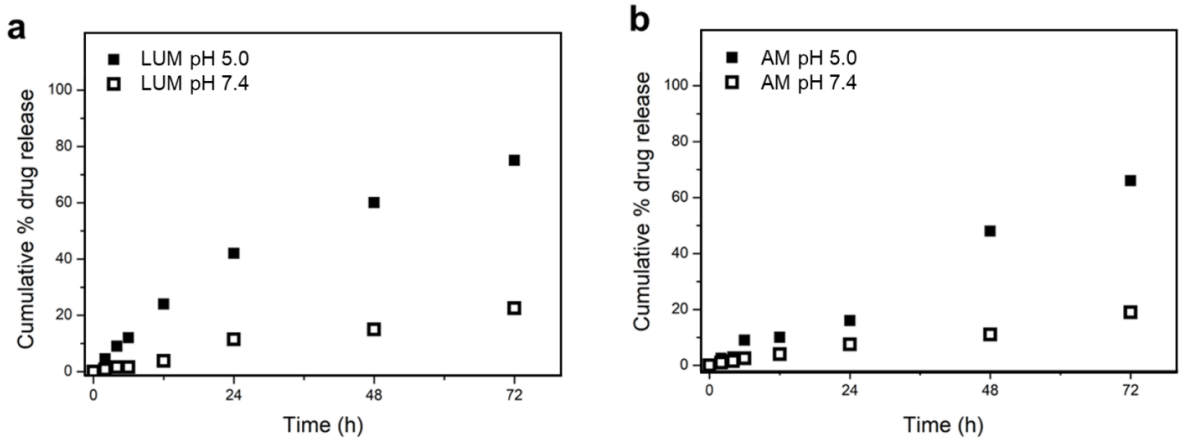

Figure 9. Cumulative % drug release of a) LUM and b) AM at pH 5 (acetate buffer) and at pH 7.4 (PBS buffer) and pH 5.0 (acetate buffer) from DLMs.

Conjugation of the targeting ligand to the polymeric prodrug. After establishing that the DLMs conjugate was kinetically and thermodynamically stable, and disassembled in response to a pH trigger, we also functionalized some of the DLMs with the peptide 'GSRSKGT' to form ligand tagged DLMs (L-DLM), to determine whether this would enhance the uptake into iRBCs. A study by Eda *et al.* evaluated the targeting efficacies of peptidic targeting ligands for *Plasmodium*-infected RBCs,[77] including 'GSRSKGT', which displayed a relatively low targeting efficacy, however, we opted to use 'GSRSKGT' because the other peptides are larger and more hydrophobic, which in our case may complicate the self-assembly process. To bioconjugate the ligand to DLMs, the *N*-terminus of the ligand was modified using succinimidyl 3-(2-pyridyldithio)propionate (SPDP) to have a pyridyl disulfide (PDS)-terminated end group. The modification reaction was

conducted at a pH of 9, which is ~2 units lower than the pK_a of the ε-amino groups, limiting interference (Scheme S6).[78] Modification of only one amino moiety was confirmed via positive mode ESI-MS and a DTT assay (see SI). Following this, the thiol protected SPDP-modified peptide was deprotected using DTT and attached to the PDS end-modified PVP block through disulfide exchange at pH 7 in PBS (Scheme 3). A ligand density of approximately 12 ± 3 mol% of the polymer chains were tethered to the peptide using the DTT assay, with SPDP terminating the remainder of PVP's end groups. The general recommendation for effective ligand densities is that overcrowding of the aggregate be avoided. Optimization of the degree of ligand functionalization should take place after the initial efficacy studies.

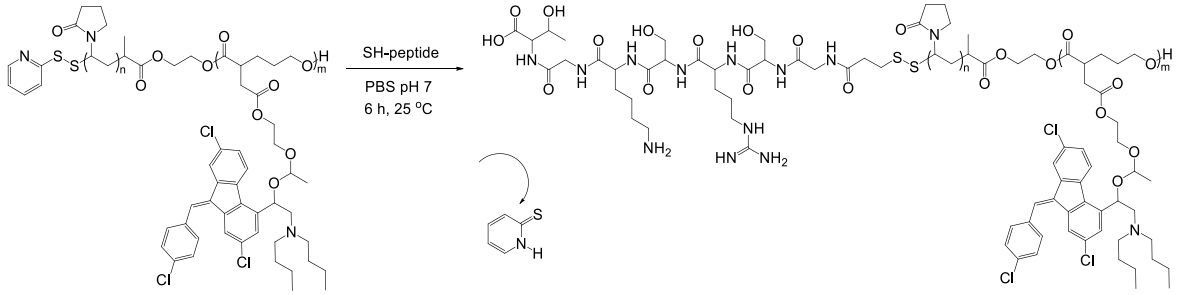

Scheme 3. Bioconjugation of the thiol terminated targeting ligand to the LUM prodrug.

Haemolytic activity. The haemolytic activity of the nanoaggregates in comparison to free AL drug was determined following a 48 h treatment with uninfected RBCs, as described by Rautenbach *et al.*[79] The AL-DLM and AL-L-DLM showed significantly decreased haemolytic activity (< 0.1%, $P < 0.05$) compared to free AL drug (~7% haemolysis) at both 5 and 10 μM (Figure 10a), with no haemolytic activity observed for EM (10 μM, results not shown). This indicates that encapsulation of free AL drug into nanoaggregates decreases the lytic activity of the drug towards uninfected erythrocytes.

Cytotoxicity. To determine if the nanoaggregates decrease the *in vitro* cytotoxicity compared to free AL drug, their respective activities against mammalian HepG2 cells was determined following a 48 h treatment at 37 °C.[80] Although free AL drug showed low cytotoxity (< 5%) at 10 μM, the

AL-DLM and AL-L-DLM nanoaggregates showed a significant decrease in their relative cytotoxicities at this concentration (< 2%, Figure 10b). No *in vitro* toxicity of the EM polymer towards mammalian HepG2 cells cytotoxicity was observed at 10 µM (results not shown).

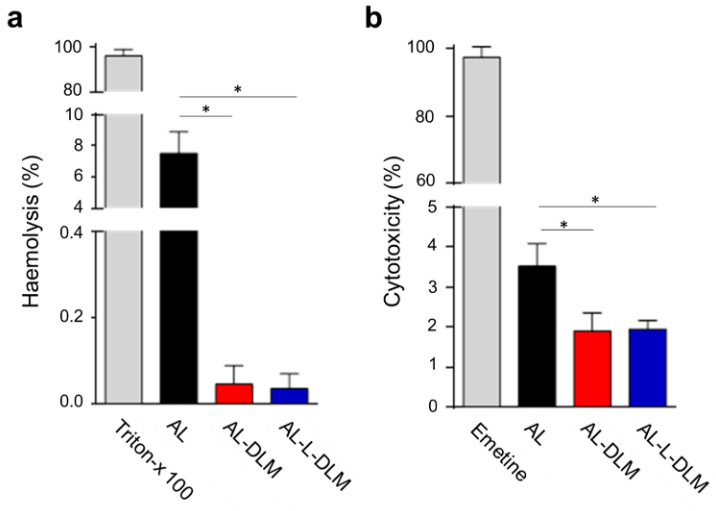

Figure 10. Haemolytic activity and cytotoxicity of free AL in comparison to AL aggregated with DLM and L-DLM at 10 µM AL. a) Haemolytic activity of free AL drug to AL-DLM and AL-L-DLM treated RBC's at 10 µM for 48 h at 37 °C with Triton-x 100 control. b) Cytotoxicity against mammalian HepG2 cells of free AL drug to AL-DLM and AL- L-DLM and L-DLMs at 10 µM with emetine as reference control drug. Results are representative of three biological replicates, n = 3, each performed as technical triplicates, ± SEM. Statistically significant differences are indicated (*P<0.05, unpaired Student's t-test).

***P. falciparum* efficacy.** The *in vitro* antimalarial activity of the nanoaggregates compared to the free AL drug against intraerythrocytic *P. falciparum* parasites were determined using an antiproliferative assay after a 96 h incubation at 37 °C under hypoxic conditions, as described.[80] The EM exhibited no antimalarial activity at 10 µM (results not shown), indicating no *in vitro* toxicity of the polymer towards intraerythrocytic *P. falciparum* parasites. Compared to the potent activity of the free AL drug (IC_{50} 0.86 ± 0.21 nM, P < 0.05, Figure 11), the nanoaggregates showed a significant ~1000× loss in *in vitro* activity against *P. falciparum* parasites: AL-DLM: IC_{50} 1.6 ±

0.59 µM and AL-L-DLM: IC_{50} 1.0 ± 0.27 µM, Figure 11. Hence, the aggregate containing the targeting ligand did not show the expected improvement in activity.

The loss in activity observed for the aggregates in comparison to free AL drug could be attributed to aggregate disassembly requiring longer incubation periods to effectively release AL (Figure 9) as compared to the duration of the *in vitro* activity experiments. *P. falciparum* parasites replicate over a 48 h developmental cycle with the food vacuole only present for 12 - 24 h. Therefore, the fact that a 72 h incubation at pH 5.0 is required to effectively release 70% of drug (Figure 9) could mean that the acid-labile release system cannot be activated in the time span of one replication cycle of the parasite. Future studies will focus on the evaluation of the cellular internalization of the nanoaggregates in the parasitic food-vacuole for effective drug release to take place. Despite the loss in activity of the free AL drug in comparison to the nanoaggregates, the decreased cytotoxicity of the nanoaggregates observed in Figure 10b, offers potential for improved selectivity of the encapsulated AL drug towards intraerythrocytic *P. falciparum* parasites if the release profile from the DLM can be adjusted.

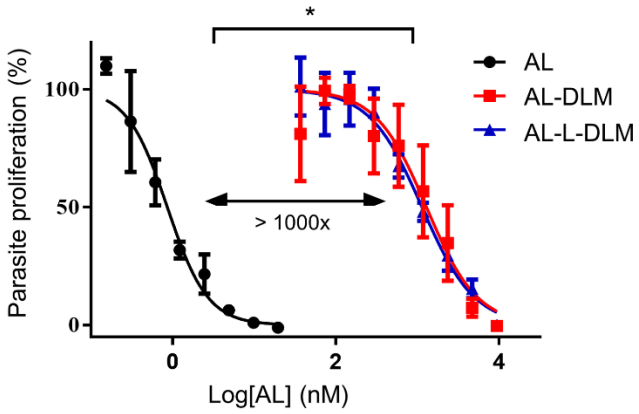

Figure 11. Dose-response curves for free AL drug, AL-DLMs and AL-L-DLMs against asexual NF54 *P. falciparum* parasites using the SYBR Green I based assay for 96 h at 37 °C. Results are representative of three independent biological replicates, n = 3, each performed in technical triplicates, ± SEM.

CONCLUSIONS

A facile route to the synthesis of a targeted, biodegradable and highly functional polymeric prodrug for combination therapy was described. A biodegradable block copolymer composed of PDS-terminated PVP and allylated poly(δ-valerolactone) was chemically functionalized in facile steps to incorporate LUM (drug 1) conjugated via an acid-labile acetal linker and a peptidic targeting ligand. Combination therapy was facilitated through the physical entrapment of AM (drug 2) within the hydrophobic domain of the prodrug micelles through self-assembly. This system self-assembled into small, uniform spherical micelles (114 nm from DLS), which is ideal in terms of size for avoiding recognition by the reticuloendothelial system (RES) and for enhancing passive accumulation in malaria-infected RBCs through the so-called new permeation pathways. The acetal-linkage served to control the drug release and disassembly of the prodrug micelles, which was accelerated under acidic conditions. The DLMs were found to be sufficiently stable for exposure *in vivo* by assessing the thermodynamic stability (CMC of 2.0 $mg \cdot mL^{-1}$) and the kinetic stability against physiologically-mimicking serum (stable for four days). AM was dispersed in the hydrophobic core of the polymeric prodrug micelles which is advantageous in terms of improving the bioavailability of the drug and its loading content within the micelle. Despite the decrease in antimalarial activity *in vitro* of the AL-DLM and AL-L-DLM nanoaggregates compared to free AL drug, the toxicity results showed that encapsulation of AL with polymers decreased both the haemolytic toxicity and HepG2 cytotoxicity in comparison to free AL. This biodegradable, highly functional polymeric prodrug is promising for the delivery of a variety of drugs intended for combination therapy and holds great potential for further development in the treatment of life-threatening diseases like malaria and others.

ASSOCIATED CONTENT

The Supporting Information is available free of charge on the ACS Publications website.

Supporting Information. Materials and methods, ^{1}H NMR spectra, SEC and ESI-MS.

Corresponding Authors

*Email: bklump@sun.ac.za, rueben@sun.ac.za

ORCID

Lisa Fortuin: 0000-0002-6911-5813

Meta Leshabane: 0000-0001-6885-1483

Rueben Pfukwa: 0000-0002-4816-2848

Dina Coertzen: 0000-0002-8408-244X

Lyn-Marie Birkholtz: 0000-0001-5888-2905

Bert Klumperman: 0000-0003-1561-274X

NOTES

The authors declare no competing financial interest.

ACKNOWLEDGEMENTS

This work is based on the research supported by the South African Research Chairs Initiative of the Department of Science and Technology (DST) and National Research Foundation (NRF) of South Africa (Grant no. 46855), SARCHI: Communities of Practice in Malaria Elimination (Grant no. 110666) and SARChI Research Chair UID 84627.

Supporting Information. Experimental materials, methods and protocols; NMR spectra; kinetic analysis; ESI-MS spectra; biological data.

REFERENCES

1. Duncan, R. The dawning era of polymer therapeutics. *Nat. Rev. Drug Discovery* **2003,** *2* (5), 347-360.
2. Hoste, K.; De Winne, K.; Schacht, E. Polymeric prodrugs. *Int. J. Pharm.* **2004,** *277* (1), 119-131.
3. Ringsdorf, H. Structure and properties of pharmacologically active polymers. *J. Appl. Polym. Sci.* **1975**, *51* (1), 135-153.
4. Kataoka, K.; Harada, A.; Nagasaki, Y. Block copolymer micelles for drug delivery: design, characterization and biological significance. *Adv. Drug Deliv. Rev.* **2012,** *64*, 37-48.
5. Kwon, G. S.; Kataoka, K. Block-copolymer micelles as long-circulating drug vehicles. *Adv. Drug Deliv. Rev.* **1995,** *16* (2), 295-309.
6. Larson, N.; Ghandehari, H. Polymeric conjugates for drug delivery. *Chem. Mater.* **2012,** *24* (5), 840-853.
7. Blanazs, A.; Armes, S. P.; Ryan, A. J. Self-Assembled block copolymer aggregates: From micelles to vesicles and their biological applications. *Macromol. Rapid Commun.* **2009,** *30* (4), 267-277.
8. Cabral, H.; Miyata, K.; Osada, K.; Kataoka, K. Block copolymer micelles in nanomedicine applications. *Chem. Rev.* **2018,** *118* (14), 6844-6892.
9. Torchilin, V. P. Micellar nanocarriers: pharmaceutical perspectives. *Pharm. Res.* **2007,** *24* (1), 1-16.
10. Kooijmans, S. A. A.; Fliervoet, L. A. L.; van der Meel, R.; Fens, M.; Heijnen, H. F. G.; van Bergen En Henegouwen, P. M. P.; Vader, P.; Schiffelers, R. M. PEGylated and targeted extracellular vesicles display enhanced cell specificity and circulation time. *J. Control. Release* **2016,** *224*, 77-85.
11. Pasut, G.; Veronese, F. M. Polymer–drug conjugation, recent achievements and general strategies. *Prog. Polym. Sci.* **2007,** *32* (8), 933-961.
12. Boyer, C.; Bulmus, V.; Davis, T. P.; Ladmiral, V.; Liu, J.; Perrier, S. Bioapplications of RAFT polymerization. *Chem. Rev.* **2009,** *109* (11), 5402-5436.
13. Gaucher, G.; Dufresne, M. H.; Sant, V. P.; Kang, N.; Maysinger, D.; Leroux, J. C. Block copolymer micelles: preparation, characterization and application in drug delivery. *J. Control. Release* **2005,** *109* (1), 169-188.
14. Giliomee, J.; Pfukwa, R.; Gule, N. P.; Klumperman, B. Smart block copolymers of PVP and an alkylated PVP derivative: synthesis, characterization, thermoresponsive behaviour and self-assembly. *Polym. Chem.* **2016,** *7* (5), 1138-1146.
15. Guinaudeau, A.; Coutelier, O.; Sandeau, A.; Mazieres, S.; Thi, H. D. N.; Le Drogo, V.; Wilson, D. J.; Destarac, M. Facile Access to Poly(N-vinylpyrrolidone)-based double hydrophilic block copolymers by aqueous ambient RAFT/MADIX polymerization. *Macromolecules* **2014,** *47* (1), 41-50.
16. Guinaudeau, A.; Mazieres, S.; Wilson, D. J.; Destarac, M. Aqueous RAFT/MADIX polymerisation of N-vinyl pyrrolidone at ambient temperature. *Polym. Chem.* **2012,** *3* (1), 81-84.
17. Pound, G.; Aguesse, F.; McLeary, J. B.; Lange, R. F. M.; Klumperman, B. Xanthate-mediated copolymerization of vinyl monomers for amphiphilic and double-hydrophilic block copolymers with poly(ethylene glycol). *Macromolecules* **2007,** *40* (25), 8861-8871.
18. Pound, G.; McKenzie, J. M.; Lange, R. F.; Klumperman, B. Polymer-protein conjugates from omega-aldehyde endfunctional poly(N-vinylpyrrolidone) synthesised via xanthate-mediated living radical polymerisation. *Chem. Commun.* **2008,** (27), 3193-3195.
19. Reader, P. W.; Pfukwa, R.; Jokonya, S.; Arnott, G. E.; Klumperman, B. Synthesis of α, ω-heterotelechelic PVP for bioconjugation, via a one-pot orthogonal end-group modification procedure. *Polym. Chem.* **2016,** *7* (42), 6450-6456.
20. Teodorescu, M.; Bercea, M. Poly(vinylpyrrolidone)–a versatile polymer for biomedical and beyond medical applications. *Polym.-Plast. Technol. Eng.* **2015,** *54* (9), 923-943.
21. Carlsen, A.; Lecommandoux, S. Self-assembly of polypeptide-based block copolymer amphiphiles. *Curr. Opin. Colloid Interface Sci.* **2009,** *14* (5), 329-339.
22. Robson Marsden, H.; Kros, A. Polymer-peptide block copolymers–an overview and assessment of synthesis methods. *Macromol. Biosci.* **2009,** *9* (10), 939-951.
23. Washington, K. E.; Kularatne, R. N.; Karmegam, V.; Biewer, M. C.; Stefan, M. C. Recent advances in aliphatic polyesters for drug delivery applications. *Wiley Interdiscip. Rev.: Nanomed. Nanobiotechnol.* **2017,** *9* (4), 1446-1462.

24. Yi, Y.; Lin, G.; Chen, S.; Liu, J.; Zhang, H.; Mi, P. Polyester micelles for drug delivery and cancer theranostics: Current achievements, progresses and future perspectives. *Mater. Sci. Eng. C* **2018,** *83* (1), 218-232.
25. Parhi, P.; Mohanty, C.; Sahoo, S. K. Nanotechnology-based combinational drug delivery: an emerging approach for cancer therapy. *Drug Discov. Today* **2012,** *17* (17), 1044-1052.
26. Sun, H.; Meng, F.; Dias, A. A.; Hendriks, M.; Feijen, J.; Zhong, Z. α-Amino acid containing degradable polymers as functional biomaterials: rational design, synthetic pathway, and biomedical applications. *Biomacromolecules* **2011,** *12* (6), 1937-1955.
27. Chang, Y.-C.; Chu, I.-M., Methoxy poly(ethylene glycol)-b-poly(valerolactone) diblock polymeric micelles for enhanced encapsulation and protection of camptothecin. *Eur. Polym. J.* **2008,** *44* (12), 3922-3930.
28. Hussein, Y. H. A.; Youssry, M. Polymeric micelles of biodegradable diblock copolymers: enhanced encapsulation of hydrophobic drugs. *Materials* **2018,** *11* (5), 688-714.
29. Lee, H.; Zeng, F.; Dunne, M.; Allen, C. Methoxy poly(ethylene glycol)-block-poly(delta-valerolactone) copolymer micelles for formulation of hydrophobic drugs. *Biomacromolecules* **2005,** *6* (6), 3119-3128.
30. Le Devedec, F.; Boucher, H.; Dubins, D.; Allen, C. Factors Controlling Drug Release in Cross-linked Poly(valerolactone) Based Matrices. *Mol. Pharmaceutics* **2018,** *15* (4), 1565-1577.
31. Najer, A.; Wu, D.; Nussbaumer, M. G.; Schwertz, G.; Schwab, A.; Witschel, M. C.; Schafer, A.; Diederich, F.; Rottmann, M.; Palivan, C. G.; Beck, H. P.; Meier, W. An amphiphilic graft copolymer-based nanoparticle platform for reduction-responsive anticancer and antimalarial drug delivery. *Nanoscale* **2016,** *8* (31), 14858-14869.
32. Parrish, B.; Emrick, T., Aliphatic polyesters with pendant cyclopentene groups: controlled synthesis and conversion to polyester-graft-PEG copolymers. *Macromolecules* **2004,** *37* (16), 5863-5865.
33. Parrish, B.; Quansah, J. K.; Emrick, T. Functional polyesters prepared by polymerization of α-allyl (valerolactone) and its copolymerization with ε-caprolactone and δ-valerolactone. *J. Polym. Sci.* **2002,** *40* (12), 1983-1990.
34. Greco, F.; Vicent, M. J., Combination therapy: opportunities and challenges for polymer–drug conjugates as anticancer nanomedicines. *Adv. Drug Deliv. Rev.* **2009,** *61* (13), 1203-1213.
35. Vinciguerra, D.; Denis, S.; Mougin, J.; Jacobs, M.; Guillaneuf, Y.; Mura, S.; Couvreur, P.; Nicolas, J. A facile route to heterotelechelic polymer prodrug nanoparticles for imaging, drug delivery and combination therapy. *J. Control. Release* **2018,** *286*, 425-438.
36. Nosten, F.; Brasseur, P. Combination therapy for malaria: the way forward? *Drugs* **2002,** *62* (9), 1315-1329.
37. Aditya, N. P.; Vathsala, P. G.; Vieira, V.; Murthy, R. S.; Souto, E. B. Advances in nanomedicines for malaria treatment. *Adv. Colloid Interface Sci.* **2013,** *201* (1), 1-17.
38. Dennis, E.; Peoples, V.; Johnson, F.; Bibbs, R.; Topps, D.; Bopda-Waffo, A.; Coats, M. Utilizing nanotechnology to combat malaria. *J. Infect. Dis.* **2015,** *57* (1), 1-6.
39. Kuntworbe, N.; Martini, N.; Shaw, J.; Al-Kassas, R. Malaria intervention policies and pharmaceutical nanotechnology as a potential tool for malaria management. *Drug Dev. Res.* **2012,** *73* (4), 167-184.
40. Movellan, J.; Urban, P.; Moles, E.; de la Fuente, J. M.; Sierra, T.; Serrano, J. L.; Fernandez-Busquets, X. Amphiphilic dendritic derivatives as nanocarriers for the targeted delivery of antimalarial drugs. *Biomaterials* **2014,** *35* (27), 7940-7950.
41. Santos-Magalhaes, N. S.; Mosqueira, V. C. Nanotechnology applied to the treatment of malaria. *Adv. Drug Deliv. Rev.* **2010,** *62* (4), 560-75.
42. Nosten, F.; Brasseur, P. Combination therapy for malaria: the way forward? *Drugs* **2002,** *62* (9), 1315-1329.
43. Ashley, E. A.; Stepniewska, K.; Lindegårdh, N.; Annerberg, A.; Kham, A.; Brockman, A.; Singhasivanon, P.; White, N. J.; Nosten, F. How much fat is necessary to optimize lumefantrine oral bioavailability? *Trop. Med. Int. Health* **2007,** *12* (2), 195-200.
44. Moad, G.; Rizzardo, E.; Thang, S. H. Living radical polymerization by the RAFT process–a third update. *Aust. J. Chem.* **2012,** *65* (8), 985-1076.
45. Pound, G.; McLeary, J. B.; McKenzie, J. M.; Lange, R. F.; Klumperman, B. In-situ NMR spectroscopy for probing the efficiency of RAFT/MADIX agents. *Macromolecules* **2006,** *39* (23), 7796-7797.
46. Kang, H. U.; Yu, Y. C.; Shin, S. J.; Kim, J.; Youk, J. H., One-pot synthesis of poly (N-vinylpyrrolidone)-b-poly (ε-caprolactone) block copolymers using a dual initiator for RAFT polymerization and ROP. *Macromolecules* **2013,** *46* (4), 1291-1295.
47. Lefay, C.; Glé, D.; Rollet, M.; Mazzolini, J.; Bertin, D.; Viel, S.; Schmid, C.; Boisson, C.; d'Agosto, F.; Gigmes, D. Block copolymers via macromercaptan initiated ring opening polymerization. *J. Polym. Sci., Part A: Polym. Chem.* **2011,** *49* (3), 803-813.
48. Willcock, H.; O'Reilly, R. K. End group removal and modification of RAFT polymers. *Polym. Chem.* **2010,** *1* (2), 149-157.

49. Molander, G. A.; Harris, C. R., Sequenced reactions with samarium (II) iodide. Tandem intramolecular nucleophilic acyl substitution/intramolecular Barbier cyclizations. *J. Am. Chem. Soc.* **1995,** *117* (13), 3705-3716.
50. Kamber, N. E.; Jeong, W.; Waymouth, R. M.; Pratt, R. C.; Lohmeijer, B. G.; Hedrick, J. L. Organocatalytic ring-opening polymerization. *Chem. Rev.* **2007,** *107* (12), 5813-5840.
51. Lohmeijer, B. G.; Pratt, R. C.; Leibfarth, F.; Logan, J. W.; Long, D. A.; Dove, A. P.; Nederberg, F.; Choi, J.; Wade, C.; Waymouth, R. M. Guanidine and amidine organocatalysts for ring-opening polymerization of cyclic esters. *Macromolecules* **2006,** *39* (25), 8574-8583.
52. Baidya, M.; Mayr, H. Nucleophilicities and carbon basicities of DBU and DBN. *Chem. Commun.* **2008,** (15), 1792-1794.
53. Carafa, M.; Mesto, E.; Quaranta, E. DBU-promoted nucleophilic activation of carbonic acid diesters. *Eur. J. Org. Chem.* **2011,** *2011* (13), 2458-2465.
54. De Rycke, N.; Couty, F.; David, O. R. Increasing the reactivity of nitrogen catalysts. *Chemistry* **2011,** *17* (46), 12852-12871.
55. Shieh, W. C.; Dell, S.; Repic, O. Nucleophilic catalysis with 1,8-diazabicyclo[5.4.0]undec-7-ene (DBU) for the esterification of carboxylic acids with dimethyl carbonate. *J. Org. Chem.* **2002,** *67* (7), 2188-2191.
56. Brown, H. A.; De Crisci, A. G.; Hedrick, J. L.; Waymouth, R. M. Amidine-mediated zwitterionic polymerization of lactide. *ACS Macro Lett.* **2012,** *1* (9), 1113-1115.
57. Li, A.; Lu, L.; Li, X.; He, L.; Do, C.; Garno, J. C.; Zhang, D. Amidine-mediated zwitterionic ring-opening polymerization of N-alkyl N-carboxyanhydride: mechanism, kinetics, and architecture elucidation. *Macromolecules* **2016,** *49* (4), 1163-1171.
58. Kurth, N.; Renard, E.; Brachet, F.; Robic, D.; Guerin, P.; Bourbouze, R. Poly (3-hydroxyoctanoate) containing pendant carboxylic groups for the preparation of nanoparticles aimed at drug transport and release. *Polymer* **2002,** *43* (4), 1095-1101.
59. Mangold, C.; Dingels, C.; Obermeier, B.; Frey, H.; Wurm, F. PEG-based multifunctional polyethers with highly reactive vinyl-ether side chains for click-type functionalization. *Macromolecules* **2011,** *44* (16), 6326-6334.
60. Cherifi, N.; Khoukh, A.; Benaboura, A.; Billon, L. Diffusion-ordered spectroscopy NMR DOSY: an all-in-one tool to simultaneously follow side reactions, livingness and molar masses of polymethylmethacrylate by nitroxide mediated polymerization. *Polym. Chem.* **2016,** *7* (33), 5249-5257.
61. Groves, P. Diffusion ordered spectroscopy (DOSY) as applied to polymers. *Polymer Chemistry* **2017,** *8* (44), 6700-6708.
62. O'Driscoll, C. M.; Griffin, B. T. Biopharmaceutical challenges associated with drugs with low aqueous solubility-the potential impact of lipid-based formulations. *Adv. Drug Deliv. Rev.* **2008,** *60* (6), 617-624.
63. Goodyer, I. D.; Pouvelle, B.; Schneider, T. G.; Trelka, D. P.; Taraschi, T. F. Characterization of macromolecular transport pathways in malaria-infected erythrocytes. *Mol. Biochem. Parasitol.* **1997,** *87* (1), 13-28.
64. Baumeister, S.; Winterberg, M.; Duranton, C.; Huber, S. M.; Lang, F.; Kirk, K.; Lingelbach, K., Evidence for the involvement of Plasmodium falciparum proteins in the formation of new permeability pathways in the erythrocyte membrane. *Mol. Microbiol.* **2006,** *60* (2), 493-504.
65. El Tahir, A.; Malhotra, P.; Chauhan, V. S. Uptake of proteins and degradation of human serum albumin by Plasmodium falciparum-infected human erythrocytes. *Malar. J.* **2003,** *2* (1), 11-19.66. Kirk, K., Membrane transport in the malaria-infected erythrocyte. *Physiol Rev* **2001,** *81* (2), 495-537.
67. Urbán, P.; Valle-Delgado, J. J.; Mauro, N.; Marques, J.; Manfredi, A.; Rottmann, M.; Ranucci, E.; Ferruti, P.; Fernàndez-Busquets, X. Use of poly(amidoamine) drug conjugates for the delivery of antimalarials to Plasmodium. *J. Controlled Release* **2014,** *177* (1), 84-95.
68. Kuntworbe, N.; Acquah, F. A.; Johnson, R.; Ofori-Kwakye, K. Comparison of the physicochemical properties and in vivo bioavailability of generic and innovator artemether-lumefantrin tablets in Kumasi, Ghana. *J. Pharm. Pharmacogn. Res.* **2018,** *6* (3), 167-178.
69. Kim, I. S.; Kim, S. H. Development of a polymeric nanoparticulate drug delivery system. In vitro characterization of nanoparticles based on sugar-containing conjugates. *Int. J. Pharm.* **2002,** *245* (1), 67-73.
70. Glavas, L.; Odelius, K.; Albertsson, A. C. Tuning loading and release by modification of micelle core crystallinity and preparation. *Polym. Adv. Technol.* **2015,** *26* (7), 880-888.
71. Gou, J. X.; Feng, S. S.; Xu, H. L.; Fang, G. H.; Chao, Y. H.; Zhang, Y.; Xu, H.; Tang, X. Decreased core crystallinity facilitated drug loading in polymeric micelles without affecting their biological performances. *Biomacromolecules* **2015,** *16* (9), 2920-2929.
72. Ray, G. B.; Chakraborty, I.; Moulik, S. P. Pyrene absorption can be a convenient method for probing critical micellar concentration (cmc) and indexing micellar polarity. *J. Colloid Interface Sci.* **2006,** *294* (1), 248-254.
73. Owen, S. C.; Chan, D. P.; Shoichet, M. S., Polymeric micelle stability. *Nano Today* **2012,** *7* (1), 53-65.

74. Liang, K.; Chung, J. E.; Gao, S. J.; Yongvongsoontorn, N.; Kurisawa, M. Highly augmented drug loading and stability of micellar nanocomplexes composed of doxorubicin and poly(ethylene glycol)-green tea catechin conjugate for cancer therapy. *Adv. Mater.* **2018,** *30* (14), 170-178.
75. Spielmann, T.; Gras, S.; Sabitzki, R.; Meissner, M. Endocytosis in plasmodium and toxoplasma parasites. *Trends Parasitol.* **2020,** *36* (6), 520-532.
76. Yayon, A.; Cabantchik, Z. I.; Ginsburg, H. Identification of the acidic compartment of plasmodium-falciparum-infected human-erythrocytes as the target of the antimalarial drug chloroquine. *EMBO J.* **1984,** *3* (11), 2695-2700.
77. Eda, K.; Eda, S.; Sherman, I. W. Identification of peptides targeting the surface of Plasmodium falciparum-infected erythrocytes using a phage display peptide library. *Am. J. Trop. Med. Hyg.* **2004,** *71* (2), 190-195.
78. Chan, A. O. Y.; Ho, C. M.; Chong, H.-C.; Leung, Y. C.; Huang, J. S.; Wong, M. K.; Che, C. M., Modification of N-terminal α-amino groups of peptides and proteins using ketenes. *J. Am. Chem. Soc.* **2012,** *134* (5), 2589-2598.
79. Rautenbach, M.; Vlok, N. M.; Stander, M.; Hoppe, H. C. Inhibition of malaria parasite blood stages by tyrocidines, membrane-active cyclic peptide antibiotics from Bacillus brevis. *Biochim. Biophys. Acta* **2007,** *1768* (6), 1488-1497.
80. Verlinden, B. K.; Niemand, J.; Snyman, J.; Sharma, S. K.; Beattie, R. J.; Woster, P. M.; Birkholtz, L. M. Discovery of novel alkylated (bis)urea and (bis)thiourea polyamine analogues with potent antimalarial activities. *J. Med. Chem.* **2011,** *54* (19), 6624-6633.

For Table of Contents Use Only

Title: "A Facile Route to Targeted, Biodegradable Polymeric Prodrugs for the Delivery of Combination Therapy for Malaria"

Author(s): Fortuin, Lisa; Leshabane, Meta; Pfukwa, Rueben; Coertzen, Dina; Birkholtz, Lyn-Marie; Klumperman, Bert